THE JOURNAL OF INVESTIGATIVE DERMATOLOGY, 69:376–378, 1977

Vol. 69, No. 4
Printed in U.S.A.

APATITE CRYSTALS IN PSEUDOXANTHOMA ELASTICUM: A COMBINED STUDY USING ELECTRON MICROSCOPY AND SELECTED AREA DIFFRACTION ANALYSIS

A. OTKJÆR-NIELSEN, M.D., E. JOHNSON, M.Sc., B. HENTZER, M.D., L. DANIELSEN, M.D., AND F. CARLSEN, M.Sc.

Department of Dermatology, University of Copenhagen, Rigshospital (AO-N, BH); Physics Laboratory II, H. C.Ørsteds Institute, University of Copenhagen (EJ, FC); Clinic of Dermatology, Municipal Hospital (LD), Copenhagen, Denmark

Calcium deposits in elastic fibers of involved skin of patients suffering from pseudoxanthoma elasticum have previously been reported. In the present work, the crystalline structure and composition were studied. Involved skin was obtained from 5 patients. Bright-field and dark-field electron microscopy and selected area electron diffraction of the calcium deposits were applied. The study demonstrates calcium apatite crystals.

Pseudoxanthoma elasticum (PXE) is a genetically determined disease involving elastic and collagen fibers in skin, eyes, and vascular tissues. Previous ultrastructural studies of the skin lesions have shown twisting and increased diameters of collagen fibrils, presence of thready masses, and calcium deposits inside and around elastic fibers [1,2]. Increased amounts of calcium salts in the skin lesions have been shown by various methods [1, 3–5]. The ultrastructure of the calcium deposits appeared as electron-dense granules and thin stripes reminiscent of apatite crystals [2].

It was the aim of the present study to demonstrate the nature of these deposits and, by using dark-field microscopy, to study the distribution of the crystals in the mineralized deposits.

MATERIALS AND METHODS

Biopsies were taken from typical PXE skin lesions in the axillary regions of 5 patients. The specimens were fixed in 6% glutaraldehyde solution with 7.5% sucrose, buffered at pH 7.4 with 0.1 M cacodylate, then osmicated, dehydrated, and embedded in Epon 812. Ultrathin sections were cut on an LKB-ultramicrotome. For bright-field and dark-field microscopy, sections were stained using a combined technique with uranyl acetate and lead citrate. To determine the crystal structure, selected area diffraction patterns were recorded from deposits in unstained specimens. The diffraction constant of the microscope was determined from diffraction patterns of evaporated, thin, polycrystalline gold films, exposed without altering the lens exitations. To establish the connection between the deposits and the diffraction rings, bright-field and tilted-beam dark-field [6] micrographs were recorded from the same areas.

A Siemens Elmiscope I microscope was used for microscopy and diffraction and a JEOL 100 U microscope for tilted beam dark-field microscopy.

Manuscript received March 29, 1977; accepted for publication April 19, 1977.

Reprint requests to: Dr. A. Otkjær-Nielsen, Department of Dermatology, Rigshospital, Blegdamsvej 9, DK-2100 Copenhagen Ø, Denmark.

Abbreviations:
PXE: pseudoxanthoma elasticum

RESULTS

Selected Area Diffraction

The identification of the calcium deposits as apatite was made from selected area diffraction patterns. Figure 1 shows a bright-field micrograph of a typical calcium deposit in an unstained specimen. An indexed selected area diffraction pattern recorded from this deposit is shown in Figure 2. The crystal lattice spacings obtained for the observable diffraction rings in Figure 2 are listed in the Table together with lattice spacings and equivalent Miller indices for calcium hydroxyapatite and calcium fluoroapatite as reported in the American Society for Testing Materials (ASTM) files.*

Bright-Field and Dark-Field Microscopy

The deposits inside the elastic fibers appeared in two zones: (1) Inside the central area, homogeneous masses of coarse granules and needles with moderate electron density appeared (Figs. 3, 4). (2) At the periphery, a narrow, highly electron-dense border containing needle-like structures was seen. The structures were probably crystals and they were arranged grossly parallel to each other (Fig. 5). In dark-field microscopy, the dense border showed no excessive contrast, complementary to that seen in bright-field microscopy, and the needle-like structures could not be resolved (Figs. 4, 5). Some deposits were divided into subunits by borders (Fig. 3).

The results obtained were the same in all patients.

DISCUSSION

In 1937, Finnerud and Nomland [4], using von Kossa's silver impregnation, showed that the elas-

* ASTM inorganic index to powder diffraction file, Powder Diffraction Index Set 17i. American Society for Testing and Materials, Philadelphia, 1967.

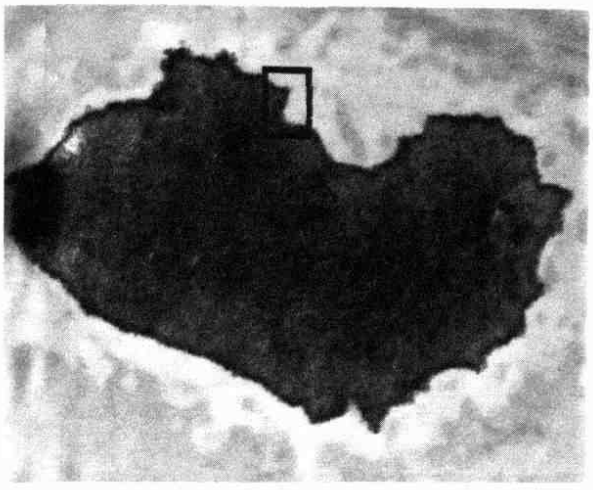

FIG. 1. Bright-field micrograph of a calcium deposit in an unstained elastic fiber of a PXE lesion. The *rectangle* indicates the area shown in Figure 5 (× 13,000).

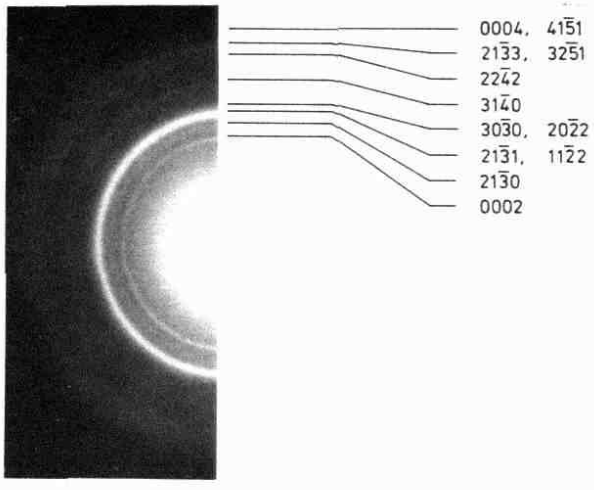

FIG. 2. Selected area diffraction pattern from the deposit shown in Figure 1. The diffraction pattern, indexed according to the Table, shows that the deposit is of apatite type. The indices refer only to the intense rings of the ASTM files.

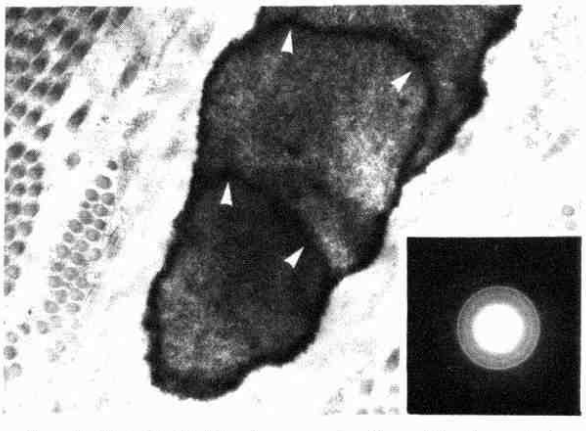

FIG. 3. Bright-field micrograph of apatite deposit in a stained elastic fiber. The deposit is subdivided by borderlines (*arrowheads*). The *inset* shows the selected area diffraction pattern of the deposit (× 11,000).

TABLE. *Experimental electron diffraction data obtained from a mineralized deposit in unstained PXE elastic fiber compared with x-ray diffraction data for calcium fluoroapatite and calcium hydroxyapatite**

ASTM Data			Experimental Data[d] d(hkil) Å
Miller indices[a] hkil	Fluoroapatite[b] d(hkil) Å	Hydroxyapatite[c] d(hkil) Å	
10$\bar{1}$0	8.12	8.17	
10$\bar{1}$1	5.25	5.26	
11$\bar{2}$0	4.684	4.72	
20$\bar{2}$0	4.055	4.07	
11$\bar{2}$1	3.872	3.88	
20$\bar{2}$1	3.494	3.51	
000$\bar{2}$	3.442	3.44	3.44
10$\bar{1}$2	3.167	3.17	
21$\bar{3}$0	3.067	3.08	3.08
21$\bar{3}$1	2.800	2.814	2.80
11$\bar{2}$2	2.772	2.778	
30$\bar{3}$1	2.702	2.720	2.68[d]
20$\bar{2}$2	2.624	2.631	
30$\bar{3}$1	2.517	2.528	
21$\bar{3}$2	2.289	2.296	
31$\bar{4}$0	2.250	2.262	2.26
22$\bar{4}$1	2.218	2.228	
31$\bar{4}$1	2.140	2.148	
30$\bar{3}$2	2.128	2.134	
11$\bar{2}$3	2.061	2.065	
40$\bar{4}$0	2.028	2.040	
20$\bar{2}$3	1.997	2.000	
22$\bar{4}$2	1.937	1.943	1.93
31$\bar{4}$2	1.884	1.890	
32$\bar{5}$0	1.862	1.871	
21$\bar{3}$3	1.837	1.841	1.83
32$\bar{5}$1	1.797	1.806	
41$\bar{5}$0	1.771	1.780	
40$\bar{4}$2, 30$\bar{3}$3	1.748	1.754	
0004, 41$\bar{5}$1	1.722	1.722	1.72
10$\bar{1}$4	1.684	1.684	

[a] The four-indices notation, commonly used for hexagonal crystal. The index i is given by i = −(h + k).

[b] ASTM card No 15-876. Calcium fluoroapatite has hexagonal crystal structure with a_0 = 9.3684 Å and c_0 = 6.8841 Å.

[c] ASTM card No 9-432. Calcium hydroxyapatite has hexagonal crystal structure with a_0 = 9.418 Å and c_0 = 6.884 Å.

[d] This ring is very broad and hence the lattice spacing is somewhat uncertain.

tic fibers in PXE lesions contained calcium salts. Later, Lobitz and Osterberg [5], by means of microincineration, found a heavy concentration of calcium in PXE skin. Blumenkrantz et al [3], by means of x-ray fluorescence analysis, confirmed this and showed a high content also of phosphorus. In 1974, Blüemcke et al [1], using x-ray microanalysis, showed that the deposits in the elastic fibers had a high content of calcium and phosphorus, whereas no other element could be detected. Our selected area diffraction analysis further shows that the deposits represent apatite, although the

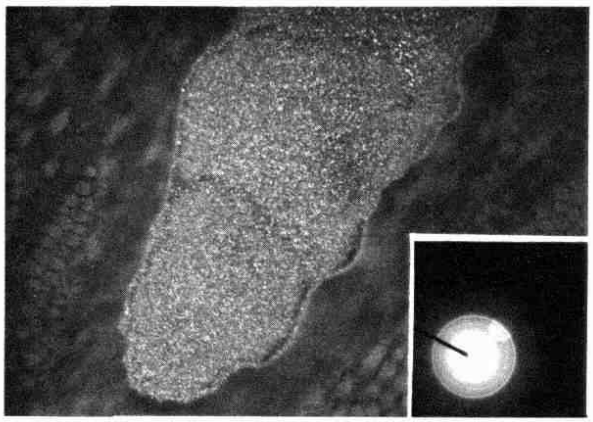

FIG. 4. Dark-field micrograph of the same apatite deposit as shown in Figure 3. The *inset* shows the selected area diffraction pattern with the segments of the diffraction rings used for forming the dark-field image, as indicated by the position of the objective aperture (× 11,000).

diffraction data alone do not allow a distinction between calcium hydroxyapatite and calcium fluoroapatite, for which an accuracy better than 0.5% is needed, while the accuracy of this study is estimated to be 1 to 2%. The size and the shape of the crystals cause a broadening of the diffraction rings, and this broadening limits the accuracy in the measurements of the ring diameters and renders weak rings invisible. It also prevents the resolution of closely spaced rings (Tab.). These problems are general features in electron diffraction work on apatite in tissue [7] as well as in x-ray diffraction work on bone apatite [8]. In contrast to our result, Martinez-Hernandez and Huffer [9] obtained no electron diffraction ring patterns from calcium deposits in affected PXE skin.

The strong bright-field contrast of the borders in stained as well as unstained specimens, cannot be explained by excessive amounts of crystalline apatite because of the noncomplementarity of the dark-field contrast. The augmented stainability and the osmiophilic properties of the borders are possibly due to the presence of organic material.

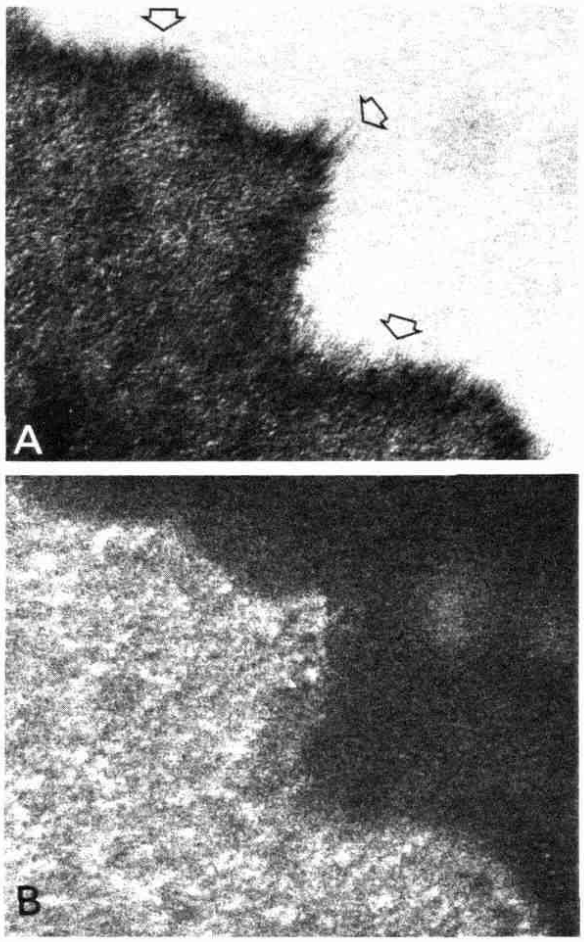

FIG. 5. High magnification bright-field (*a*) and dark-field (*b*) micrographs from the area indicated by the rectangle in Figure 1. Needle-like structures are seen protruding from the border (*arrows*) (× 80,000).

REFERENCES

1. Blëmcke S, Langness U, Liesegang B, Fooke-Achterrath M, Thiel HJ: Light and electron microscopic and element analysis of pseudoxanthoma elasticum. Beitr Pathol 152:179–199, 1974
2. Danielsen L, Kobayasi T, Larsen HW, Midtgård K, Christensen HE: Pseudoxanthoma elasticum. A clinicopathological study. Acta Derm Venereol (Stockh) 50:355–373, 1970
3. Blumenkrantz N, Danielsen L, Jørgensen K: X-ray fluorescence analysis of skin in pseudoxanthoma elasticum. Acta Derm Venereol (Stockh) 54:129–132, 1974
4. Finnerud CW, Nomland R: Pseudoxanthoma elasticum. Proof of calcifications of elastic tissue, occurrence with and without angoid streaks of the retina. Arch Dermatol 35:653–662, 1937
5. Lobitz WC, Osterberg AE: Pseudoxanthoma elasticum; microincineration. J Invest Dermatol 15:297–298, 1950
6. Heidenreich RD: Fundamentals of transmission electron microscopy. Monographs and text *in* Physics and Astronomy Series, vol XIII. New York, John Wiley, Interscience, 1964
7. Anderson HC: Vesicles associated with calcification in the matrix of epiphyseal cartilage. J Cell Biol 41:59–72, 1969
9. Eanes ED: X-ray diffraction of vertebrate hard tissue, Biological Mineralization. Edited by I. Zipkin. New York, London/Sydney/Toronto, John Wiley, 1973, pp 227–000
10. Martinez-Hernandez A, Huffer WE: Pseudoxanthoma elasticum: dermal polyanions and the mineralization of elastic fibres. J Lab Invest 31:181–186, 1974